Molecular Therapy
Methods & Clinical Development
Original Article

Temporary Reduction of Membrane CD4 with the Antioxidant MnTBAP Is Sufficient to Prevent Immune Responses Induced by Gene Transfer

Sylvie Da Rocha,[1] Jérémy Bigot,[1] Fanny Onodi,[1] Jérémie Cosette,[2] Guillaume Corre,[1] Jérôme Poupiot,[1] David Fenard,[1] Bernard Gjata,[2] Anne Galy,[1] and Thi My Anh Neildez-Nguyen[1]

[1]Ecole Pratique des Hautes Etudes, PSL Research University, INTEGRARE UMR_S951, INSERM, Généthon, Univ-Evry, 91002 Evry, France; [2]Généthon, UMR_S951, 91002 Evry, France

Unexpectedly, the synthetic antioxidant MnTBAP was found to cause a rapid and reversible downregulation of CD4 on T cells *in vitro* and *in vivo*. This effect resulted from the internalization of membrane CD4 T cell molecules into clathrin-coated pits and involved disruption of the CD4/p56^{Lck} complex. The CD4 deprivation induced by MnTBAP had functional consequences on CD4-dependent infectious processes or immunological responses as shown in various models, including gene therapy. In cultured human T cells, MnTBAP-induced downregulation of CD4 functionally suppressed gp120- mediated lentiviral transduction in a model relevant for HIV infection. The injection of MnTBAP in mice reduced membrane CD4 on lymphocytes *in vivo* within 5 days of treatment, preventing OVA peptide T cell immunization while allowing subsequent immunization once treatment was stopped. In a mouse gene therapy model, MnTBAP treatment at the time of adenovirus-associated virus (AAV) vector administration, successfully controlled the induction of anti-transgene and anti-capsid immune responses mediated by CD4$^+$ T cells, enabling the redosing mice with the same vector. These functional data provide new avenues to develop alternative therapeutic immunomodulatory strategies based on temporary regulation of CD4. These could be particularly useful for AAV gene therapy in which novel strategies for redosing are needed.

INTRODUCTION

Mn(III) tetrakis (4-benzoic acid) porphyrin chloride (MnTBAP) is a cell-permeable synthetic antioxidant with superoxide dismutase-like activity. This molecule neutralizes superoxide[1] in both extracellular and intracellular compartments.[2] Tested *in vivo*, MnTBAP is non-immunogenic, is non-toxic, and shows significant therapeutic benefits in diminishing inflammation in various models of injuries[3,4] or of organ transplantation,[5] or by reducing effector immune responses against a virus challenge.[6] In such models, the effects of MnTBAP have been attributed to reactive oxygen species (ROS) inhibition, which is its main mechanism of action. However, previous results from our laboratory suggested that MnTBAP could also act on T cells directly. Indeed, we observed that the conversion of naive CD4$^+$ T lymphocytes into Foxp3$^+$ regulatory T cells (Tregs) was hampered in the presence of 200 μM MnTBAP *in vitro*.[7] This prompted us to examine in greater detail the effects of MnTBAP on CD4$^+$ T cells. In the present study, we report for the first time that MnTBAP, can reversibly downregulate the CD4 molecules on T cells. As a primary receptor for HIV-1, CD4 is one of the most studied molecules in the human body. The CD4 T cell-surface glycoprotein mediates optimal T cell receptor (TCR) signaling during major histocompatibility complex (MHC) class II (MHCII) antigenic activation by helping in *Src*-tyrosine kinase p56^{Lck} recruitment[8] to facilitate the activation of helper T cells. Interactions between CD4 and p56^{Lck} stabilize CD4 at the plasma membrane by anchoring CD4 into distinct microvilli microdomains that constitute the primary contacts between T cells and antigen-presenting cells (APCs).[9] A tight regulation of CD4 cell-surface expression is essential for adaptive immunity, as it ensures prospective scanning of MHCII by CD4 on the surface of APCs, which is pivotal for T cell priming,[9] and enables a productive signal transduction during T cell activation. It is well established that CD4$^+$ T cells also regulate the pathogenesis of autoimmune diseases, allergies, graft- versus host disease, and rejection processes in organ transplant.[10–13] Furthermore, CD4$^+$ T cells, which are essential for protective and memory immunity against viruses initiated by infection or by vaccination,[14] are also key players in the induction of adverse immune responses following viral gene transfer therapies.[15,16] Thus, to gain insights in the effects of MnTBAP, we explored the mechanism of CD4 deprivation at the cell surface of T cells upon MnTBAP treatment and examined the functional effects on CD4-dependent T cell functions.

Indeed, we demonstrate here that MnTBAP rapidly and reversibly downregulates CD4 on T cells, disrupting the CD4/p56^{Lck} complex.

Received 20 June 2019; accepted 29 June 2019;
https://doi.org/10.1016/j.omtm.2019.06.011.

Correspondence: Anne Galy, UMR_S951, Généthon, 1 bis rue de l'Internationale, 91000 Evry, France.
E-mail: galy@genethon.fr
Correspondence: Thi My Anh Neildez-Nguyen, Ecole Pratique des Hautes Etudes, PSL Research University, UMR_S951, Généthon, 1 bis rue de l'Internationale, 91002 Evry, France.
E-mail: thi-my-anh.neildez@ephe.psl.eu

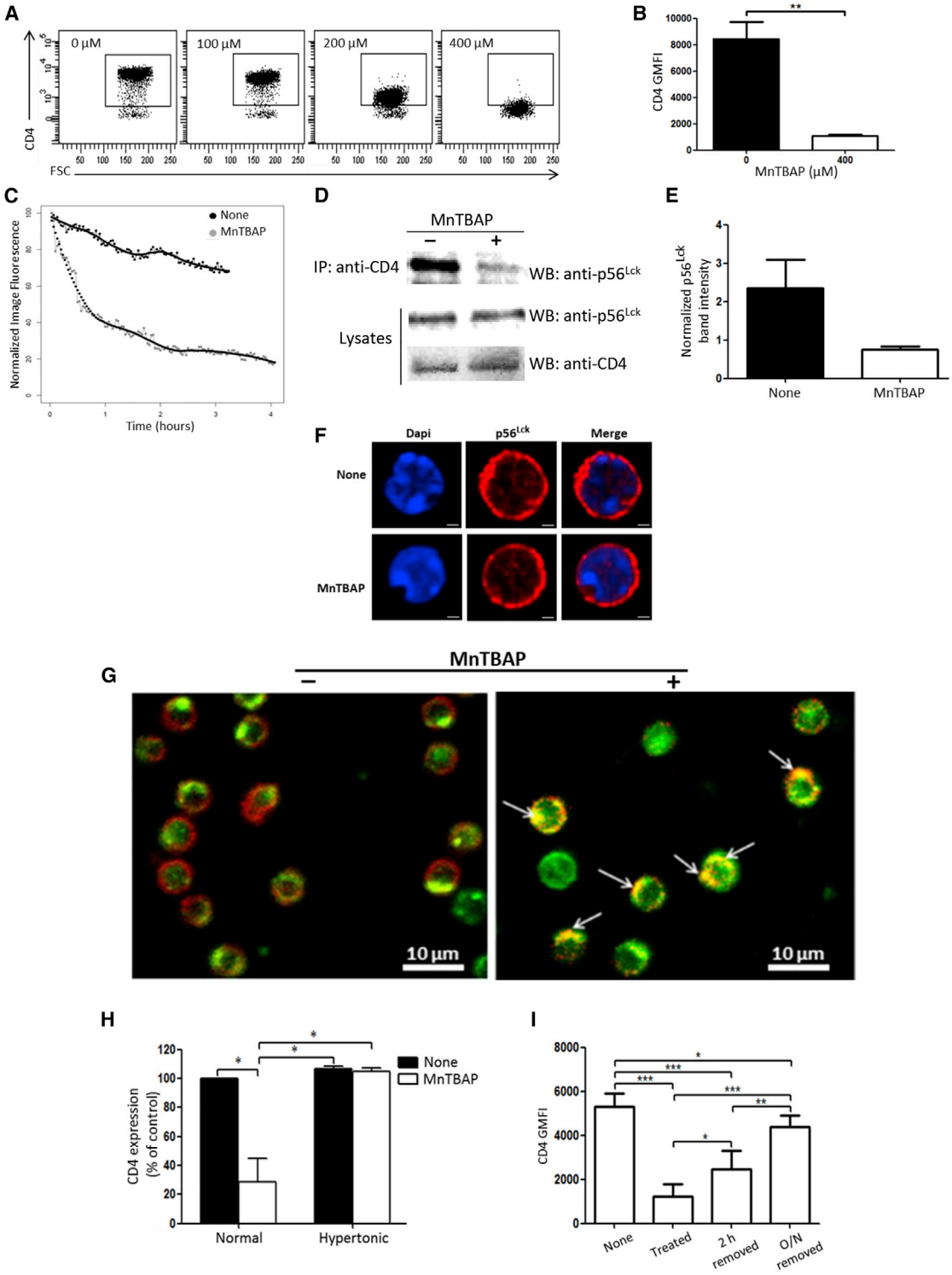

Figure 1. MnTBAP-Induced CD4 Reversible Internalization Mechanism

(A) CD4$^+$ T cells isolated by negative selection from C57BL/6 mouse splenic cell suspensions were cultured for 2 h in complete medium with increasing doses of MnTBAP (0 to 400 μM), and then analyzed by flow cytometry for CD4 expression on live splenic T cells. Data are representative of two independent experiments. (B) Graph indicating CD4 GMFI (geometric mean fluorescence intensity) on splenic CD4$^+$ T cells after treatment for 2 h with or without MnTBAP at 400 μM. (n = 4 independent experiments).

(legend continued on next page)

MnTBAP-treated cells cannot be transduced with gp120-mediated lentiviral vectors. A short MnTBAP treatment at the time of antigen priming provokes immune unresponsiveness to OVA peptide immunization and reduces specific immunological responses to adeno-associated viral vector (AAV) gene transfer. This new immunomodulatory feature of MnTBAP could be exploited to provide short-term treatment for long-term benefit in a large set of therapeutic or immunopathological conditions.

RESULTS

CD4 at the Cell Surface of T Cells Is Reversibly Internalized upon MnTBAP Treatment

To study the effects of MnTBAP on $CD4^+$ T cells, purified splenic $CD4^+$ T cells from C57BL/6 mice were treated *in vitro* for 2 h with increasing doses of MnTBAP (100–400 μM). A gradual and dose-dependent decrease of the CD4 cell-surface co-receptor was observed, with almost complete disappearance of the $CD4^+$ T cell population at the highest dose of MnTBAP tested (Figure 1A). At 400 μM, MnTBAP reduced by 8-fold the expression of CD4 at the surface of T lymphocytes (Figure 1B). This effect was not due to the induction of cell death, as measured by eFluor 780 positivity (Figure S1A). Subsequent experiments were conducted with 400 μM MnTBAP, which triggered consistently high and non-toxic loss of CD4 T cell-surface molecules. The kinetics of CD4 down-modulation by MnTBAP, investigated with time-lapse microscopy recordings over a period of 4 h of treatment, showed a rapid drop of fluorescence starting sooner than 2 min with sustained decay (Figure 1C, gray line) compared to control (Figure 1C, black line). Downregulation was maximal by 2 h of MnTBAP treatment, reaching a half-time (50% decrease of cell-surface CD4) of approximately 30 min. The CD4 downregulation was accompanied by the dissociation of the CD4/$p56^{Lck}$ complex in the cells. Less $p56^{Lck}$ was coprecipitated with CD4 in splenic T lymphocytes after 2 h of treatment with MnTBAP compared to controls (Figure 1D), whereas similar amounts of $p56^{Lck}$ and CD4 were detected on immunoblots of whole-cell lysates ("Lysates") from cells treated with or without MnTBAP (Figure 1D). Indeed, more than 3 times fewer $p56^{Lck}$ molecules were CD4 associated after MnTBAP treatment (Figure 1E). In naive murine $CD4^+$ T cells, $p56^{Lck}$ was localized to the cytosol and at the plasma membrane, and $p56^{Lck}$ localization did not change with MnTBAP treatment (Figure 1F). However, the distribution of CD4 molecules on $CD4^+$ T cells was dramatically affected by MnTBAP treatment. In sharp contrast with the control condition in which the CD4 molecules were globally distributed throughout the cell-surface membrane (Figure S1B, None), MnTBAP induced the disappearance of CD4 from the cell surface and caused its redistribution in vesicles near the cell membrane (white arrowheads) and in the cell center (red arrowhead) (Figure S1B, MnTBAP). The internalization of CD4 was accompanied by its incorporation into clathrin-coated pits,[17] as evidenced by CD4 and clathrin immunostaining and confocal microscopy analysis (Figure 1G). Untreated T lymphocytes displayed CD4 at the cell surface defining their shape (Figure 1G, left, red signal) whereas clathrin was on the inside face of the membrane (Figure 1G, left, green signal). In MnTBAP-treated cells, most cells had lost CD4 cell-surface expression in favor of a colocalization with clathrin molecules (Figure 1G, right, yellow spots; Figure S1C, Merge). Further evidence that the MnTBAP-induced CD4 internalization is dependent on the formation of clathrin-coated pits was provided by experiments in hypertonic conditions. Hypertonic cell-culture medium containing 0.45 M sucrose blocks clathrin-dependent endocytosis[18] and prevented the CD4 downregulation induced by MnTBAP (Figure 1H, Hypertonic), whereas CD4 could be internalized in iso-osmotic medium (Figure 1H, Normal). Many of the receptors internalized by clathrin-coated pits are recycled to the cell surface and re-used up to several hundred times by the cells.[19] Reportedly, in transfected 293T cells, about 45% of internalized CD4 recycled back to the cell surface within 10 min.[20] As expected from recycling biology, CD4 internalization into clathrin-coated pits induced by MnTBAP was reversible (Figure 1I): while 2-h treatment ("Treated") reduced almost 80% of CD4 cell-surface

(C) Time-lapse analysis of CD4 cell surface over time decline on $CD4^+$ T cells. After CFSE and CD4 staining, splenic $CD4^+$ T cells were incubated in the absence or presence of MnTBAP and subjected to live-cell time-lapse image acquisition every 120 s for 4 h. CD4 fluorescence intensities, normalized to the maximum fluorescence measured at t0, are reported for each condition. One representative experiment out of two is indicated. (D) MnTBAP induces disruption of the CD4/$p56^{Lck}$ complex. Protein extracts were prepared from splenic $CD4^+$ T cells after treatment for 2 h with or without MnTBAP. Crude extracts were subjected to CD4 immunoprecipitation (IP), followed by western blotting and immunodetection analysis with anti-$p56^{Lck}$. The $p56^{Lck}$ and CD4 expression levels were also analyzed in whole-cell lysates (Lysates) as controls for the quantities of the proteins of interest before immunoprecipitation. Lysates either in the absence or in the presence of MnTBAP presented approximately equal amounts of $p56^{Lck}$ and CD4. Images are representative of two independent experiments. (E) Graph of $p56^{Lck}$ band intensities detected on CD4 immunoprecipitated materials and normalized with the corresponding band in the lysates. Data are representative of two independent experiments. (F) Confocal microscopy analysis of $p56^{Lck}$ distribution in splenic $CD4^+$ T cells after treatment for 2 h with or without MnTBAP. The red fluorescence (Alexa Fluor 594) signal localizes $p56^{Lck}$ (middle panels), while the blue fluorescence (DAPI) counterstains the nuclei (left panels). Merged images of $p56^{Lck}$ and DAPI-stained nuclei are shown in the right panels. Scale bars, 1 μm. (G) CD4 internalization by a clathrin-mediated endocytosis. Murine splenic $CD4^+$ T cells were cultured for 2 h with or without MnTBAP and then were collected and subjected to immunostaining with anti-CD4 (red signal) and anti-clathrin (green signal) antibodies. Arrows indicate colocalization of CD4 and clathrin resulting in yellow spots. Scale bars, 10 μm. (H) Evidence for clathrin-mediated endocytosis of CD4 molecules. Murine splenic $CD4^+$ T cells were cultured for 2 h with or without MnTBAP in either complete medium (Normal) or hypertonic sucrose medium (Hypertonic) to inhibit specifically clathrine-dependent endocytosis. Cells were then collected and subjected to CD4 cell-surface expression analysis by flow cytometry. Results are expressed as CD4 expression relative to control (complete medium without MnTBAP; Normal), which is defined as 100%. (I) MnTBAP-induced CD4 internalization is reversible. Murine splenic $CD4^+$ T cells were cultured for 2 h with or without MnTBAP. Cells were then stained with Fixable Viability Dye-eFluor 780 (None), stained with anti-CD4-Pacific Blue and fixed (Treated), or washed to remove MnTBAP and put back in culture for either an additional 2 h (2 h removed) or overnight (O/N removed) and finally stained as described earlier and fixed. Fixed cells in all conditions were analyzed by flow cytometry for their CD4 expression, reported on the graph as CD4 GMFI. Cells in the cultures without MnTBAP (None, control) are set at 100% (n = 3 independent experiments). Statistical analyses in (B), (H), and (I) were performed using the Mann-Whitney test. *$p < 0.05$; **$p < 0.005$; ***$p < 0.0001$.

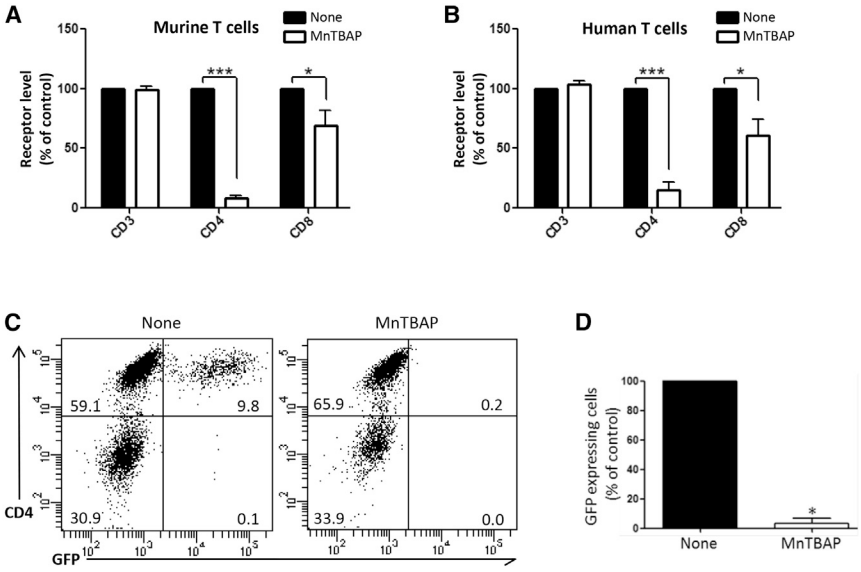

Figure 2. MnTBAP Induces Dramatic Loss of CD4 on the Surface of Murine and Human T Lymphocytes and Inhibits Transduction of Human T Lymphocytes by Lentiviral Vectors Pseudotyped with $gp120_{HXB2}$-env

(A and B) MnTBAP effect on murine (A) and human (B) T lymphocyte receptor level. Murine splenic (A) and human peripheral blood (B) cells were treated for 2 h with or without MnTBAP and then analyzed by flow cytometry for cell-surface CD3, CD4, and CD8 expression on live cells. The results of geometric means of fluorescence for each receptor are expressed relative to the corresponding values of the control non-treated cells (None, arbitrarily set at 100%); n = 3–4 independent experiments. For each receptor, statistical comparisons between untreated and treated cells were made using the Mann-Whitney test. (C) $CD3^+$ T cells from human peripheral blood were transduced in the absence or presence of 400 μM MnTBAP on retronectin-coated plates, with $gp120_{HXB2}$-env pseudotyped lentiviral vectors expressing GFP reporter gene. Transduction efficiency was assessed by flow cytometry via GFP expression 72 h post-transduction. Representative CD4/GFP dot plots are shown, with inset numbers indicating the percentage of cells in each quadrant. (D) Normalized percentages of GFP^+ cells obtained 72 h post-transduction. The percentage of GFP^+ cells in the cultures without MnTBAP (None, control) is set at 100% (n = 4 independent experiments). Statistical analysis in (D) was performed using paired t test. *$p < 0.05$; ***$p < 0.0001$.

expression, washing to remove MnTBAP and culture of T lymphocytes for an additional 2 h ("2 h removed") or overnight ("O/N removed") permitted the gradual recovery of 53% and 83% of the initial CD4 expression, respectively.

MnTBAP Dramatically Reduces the Cell-Surface CD4 on Murine and Human T Lymphocytes and Prevents gp120-Mediated Entry into Human T Cells

The levels of CD4 on murine and human T lymphocytes were similarly affected by 2-h treatment with 400 μM MnTBAP, with a 92% and 85% decrease compared to control non-treated cells for murine and human T cells, respectively (Figures 2A and 2B). MnTBAP also reduced the cell-surface CD8 by a 30% and 40% decrease compared to control non-treated cells for murine and human T cells, respectively. No alteration of CD3 expressions was observed with MnTBAP treatment (Figures 2A and 2B). Since CD4 is the primary entry receptor for HIV and mediated by gp120-CD4 interactions, we evaluated the functional consequences of MnTBAP-induced CD4 cell-surface decline in a model of HIV infection. We tested the transduction of primary human $CD3^+$ T lymphocytes by $gp120_{HXB2}$-enveloped ($gp120_{HXB2}$-env) lentiviral vectors encoding GFP that transduce specifically $CD4^+$ T cells (None, in Figure 2C, left panel). MnTBAP treatment strongly prevented virus transduction in all cells (MnTBAP, in Figure 2C, right panel, and Figure 2D) in coherence with the reduced membrane CD4 described earlier (Figure 2B). Moreover, once again, we emphasize the reversibility effect of MnTBAP, as shown in Figure 1I, since 72 h after the MnTBAP removal, treated human T lymphocytes (MnTBAP, in Figure 2C, right panel) expressed the cell-surface CD4 to levels similar to that of the control non-treated cells (None, in Figure 2C, left panel).

A Short MnTBAP Treatment Renders the Immune System Temporarily Inoperative *In Vivo*

To examine whether MnTBAP could have a functional effect via CD4 *in vivo*, we used a well-characterized CD4-dependent murine immunization model with MHCII-restricted OVA peptides. In addition, $CD8^+$ T cell responses were also determined in this model by the use of MHCI-specific peptides. MnTBAP is injectable and has already been administered to mice for its anti-oxidant effects.[3–5] Prior published data from a patent (U.S. patent no. 8598150 B1, 2013) provided indication on the effective and toxic ranges of MnTBAP in mice. However, a protocol for the use of MnTBAP *in vivo* to downregulate CD4 was not known and had to be established. Using a high-performance liquid chromatography (HPLC) technique,[21] we determined that the plasma concentration of MnTBAP in C57BL/6 mice rapidly declined over time after intraperitoneal (i.p.) injection of 80 mg/kg (data not shown), prompting a multi-administration schedule. The first protocol tested aimed to inhibit $CD4^+$ T cells prior to, and after exposure to, the antigen in order to demonstrate the possibility of interfering with $CD4^+$ T cell-mediated responses after immunization. This protocol included one MnTBAP injection 2 h prior to immunization and four daily injections post-immunization (Figure 3A). Immunization was conducted through subcutaneous (s.c.) OVA peptides or PBS injections with an adjuvant (IFA) (Figure 3A). Interferon gamma enzyme-linked immunospot assay (IFN-γ ELISPOT) measurements of T cell activation were performed 8 days after OVA immunization, by *in vitro* stimulation of splenic cells with $OVA_{257–264}$ or $OVA_{323–339}$, used to detect specifically cytolytic $CD8^+$ and $CD4^+$ T cell responses, respectively. In control mice not treated with MnTBAP (PBS + OVA/IFA), potent OVA-specific $CD4^+$ and $CD8^+$ IFN-γ-producing T cell responses were measured

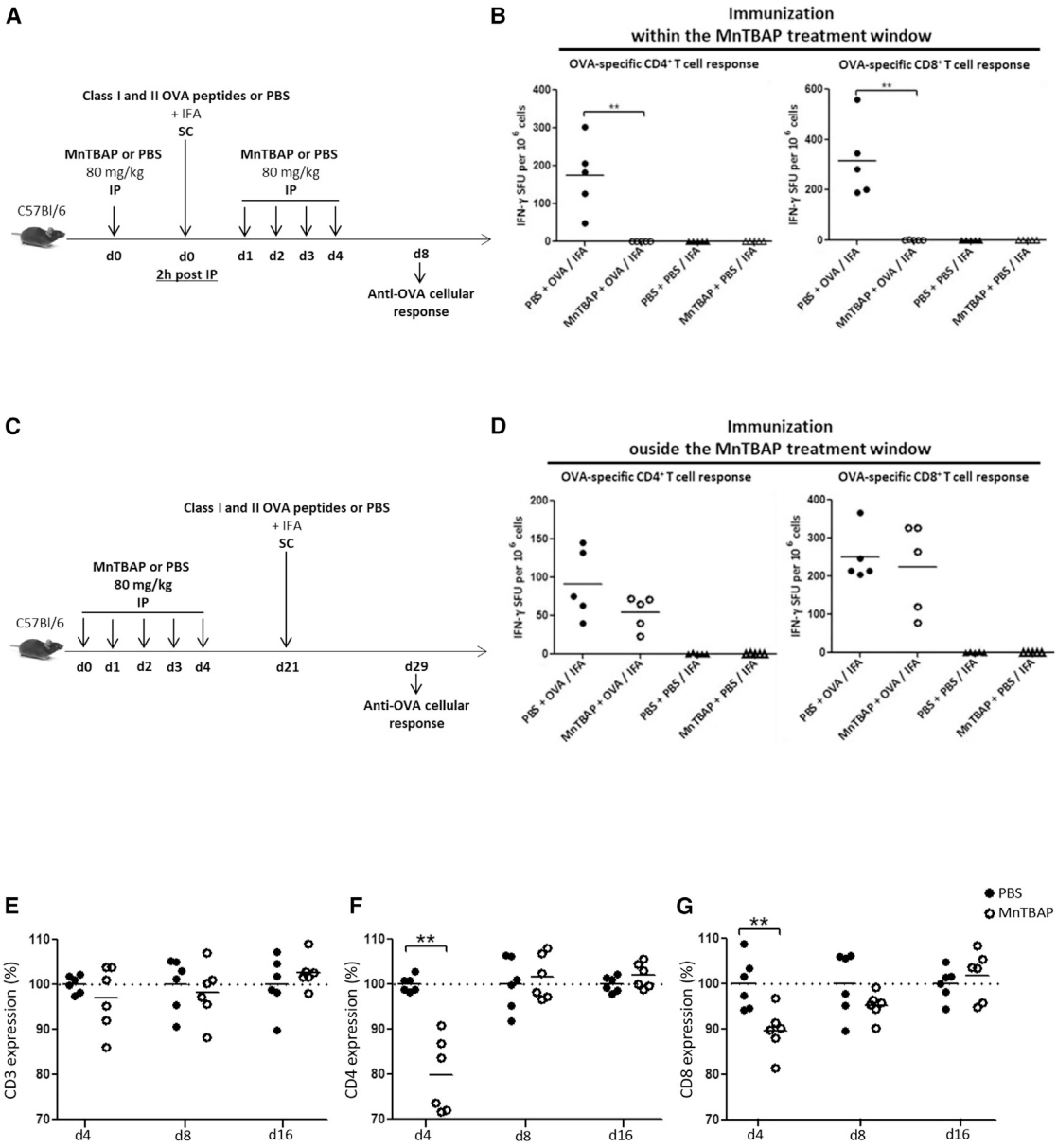

Figure 3. Temporary *In Vivo* Inhibition of the Immune System by MnTBAP

(A) Schema of OVA peptide immunization within the MnTBAP treatment window. C57BL/6 mice received i.p. multi-injections of MnTBAP or an equivalent volume of PBS (80 mg/kg daily during 5 days, day 0 to day 4). Two hours after the first i.p. injection of MnTBAP or PBS, mice received s.c. immunizations of 100 μg each of class I and class II OVA peptides or PBS emulsified with IFA. Splenic cells were harvested 8 days after immunization (day 8) to measure $CD4^+$ and $CD8^+$ T cell responses by IFN-γ ELISPOT, following *in vitro* stimulation with $OVA_{323–339}$ and $OVA_{257–264}$ peptides, respectively. (B) OVA-specific $CD4^+$ (left panel) and $CD8^+$ (right panel) T cell responses. MnTBAP (open symbols) or PBS (closed symbols) i.p. injections and OVA peptide (circles) or PBS (triangles) s.c. immunizations. Each symbol represents IFN-γ spot-forming units (duplicate measures) in each mouse. Horizontal bars indicate the average values. (C) Schema of OVA peptide immunization outside the MnTBAP treatment window. Immunizations were as described earlier, with one difference: that mice received s.c. injections of OVA peptides or PBS, emulsified with IFA, 21 days after the first i.p. injection of MnTBAP or PBS. Splenic cells were harvested 8 days after immunization (day 29) to measure $CD4^+$ and $CD8^+$ T cell responses by IFN-γ ELISPOT, following *in vitro* stimulation with $OVA_{323–339}$ and $OVA_{257–264}$ peptides, respectively. (D) OVA-specific $CD4^+$ (left panel) and $CD8^+$ (right panel) T cell responses. MnTBAP (open symbols) or PBS (closed symbols) i.p. injections and OVA peptide (circles) or PBS (triangles) s.c. immunizations. Each symbol represents IFN-γ spot-forming units (duplicate measures) of each mouse. Horizontal bars indicate the average values. Data represent one experiment with five mice per group. (E–G) MnTBAP effect on cell-surface levels of CD3 (E), CD4 (F),

(legend continued on next page)

in the spleen of mice immunized with OVA as expected (Figure 3B). In contrast, no OVA-specific T cell immune responses were mounted in OVA-immunized mice treated with MnTBAP (MnTBAP + OVA/IFA), similar to control mice that were not immunized (PBS + PBS/IFA and MnTBAP + PBS/IFA). Thus, MnTBAP reduced both $CD4^+$ and $CD8^+$ T cell-mediated immunity following immunization. As these effects could be potentially immunosuppressive, a second protocol was designed to confirm the presumed reversible effect of MnTBAP by immunization with OVA outside the MnTBAP treatment window (Figure 3C). Mice injected with peptides 21 days post-MnTBAP administration (Figure 3C) were capable of mounting OVA-specific $CD4^+$ and $CD8^+$ IFN-γ T cell responses as high as those in the PBS group (Figure 3D). Splenic cells from PBS- or MnTBAP-treated mice were assayed by flow cytometry for cell-surface expression of CD3, CD4, and CD8 (Figures 3E–3G). Significant downregulation of CD4 and CD8 by MnTBAP were shown to occur *in vivo* at day 4, with cell-surface levels being ≈80% and 90% of those seen in PBS-treated mice, respectively (Figures 3F and 3G). The CD4 and CD8 cell-surface levels recovered at day 8 and day 16 to levels similar to those of control mice, whereas the CD3 level remained unchanged with MnTBAP treatment throughout the study (Figure 3E).

Taken together, we show that, in mice, adaptive T cell immune responses to highly immunogenic antigens can be quelled by MnTBAP, provided that the vaccine is administrated within the MnTBAP treatment window in which a major effect on $CD4^+$ T cells and a weaker effect on $CD8^+$ T cells are observed. These results prompted us to investigate whether MnTBAP could be exploited in a challenging and therapeutic application involving strong $CD4^+$ T cell-mediated immune responses.

MnTBAP Treatment Prevents Anti-transgene Immune Responses following Intramuscular rAAV Gene Transfer in Mice, Reducing $CD8^+$ T Cell Infiltration and Muscle Damage

In gene therapy, cellular immune responses can be readily induced against transgene and vector following recombinant AAV (rAAV) gene transfer in mice. These immune responses lead to the loss of transgene-expressing cells and to the production of neutralizing antibodies against the rAAV capsid that prevent redosing the mice with the same vector. We previously established an immunogenic gene transfer model to follow transgene-specific $CD4^+$ and $CD8^+$ T cell responses following intramuscular (i.m.) rAAV1-mediated gene delivery in mice. In this model, the transgene is expressed at the membrane of skeletal muscle fibers and consists of the human α-sarcoglycan (SGCA) gene fused to the male HY gene sequences (SGCA-HY). When expressed from a cytomegalovirus (CMV) promoter, this transgene is highly immunogenic in female mice that are not tolerant to the male HY antigen. The i.m. injection of low doses of rAAV1 ($2–5 \times 10^9$ viral genomes [vgs] per injection, i.e., about 10^{11} vg/kg) was sufficient to induce effector anti-transgene and anti-capsid T cell responses that are highly dependent on MHCII-dependent antigenic presentation and activation of transgene-specific CD4+ T cells.[15,22] To determine whether MnTBAP could affect T and B cell immune responses induced by rAAV1 i.m. gene transfer, we implemented the protocol of MnTBAP administration used for OVA immunization (Figure 4A). The CMV-driven SGCA-HY transgene (rAAV1_CMV_SGCA_HY, 2.5×10^9 vg per mouse) was delivered via i.m. injection in left tibialis anterior (TA) muscle, in the time window of MnTBAP administration, 2 h after the first MnTBAP injection (Figure 4A). Since MnTBAP is primarily a well-known antioxidant molecule, its contribution to reduce inflammation by the innate immune system, at the site of vector delivery, should also decrease the establishment of subsequent adaptive immunity. Indeed, there was no significant inflammation detected by light emission in the left PBS injected-TA of animals treated with PBS and MnTBAP, as shown in Figure S2A, following a chemical reaction of ROS with the luminol-based substrate L-012 (Figure 4A).

Moreover MnTBAP-treated mice presented clearly a very low total ROS level at the i.p. site of multi-injection, compared to PBS-treated mice (Figure S2A). In a similar way, rAAV1-injected muscles of MnTBAP-treated mice presented 4 days post-vector injection with a reduced inflammation compared to that of their control counterparts (Figures S2B and S2C). At the histological level 15 days after gene transfer, a reduced muscular inflammation in MnTBAP-treated mice (MnTBAP/rAAV1) coincided with the presence of a high number of preserved myofibers shown by H&E staining, strongly contrasting with the tissue destruction and generalized centro-nucleation of myofibers reflecting extensive tissue regeneration in control mice (PBS/rAAV1) (Figures 4B, left panels, and 4C). At the same time point, the i.m. administration of rAAV1_CMV_SGCA_HY vector in MnTBAP-treated mice led also to a lower level of $CD8^+$ T cell infiltrate, but to robust and persistent SGCA transgene expression (Figures 4D and 4E, respectively), as measured by RT-PCR in TA of MnTBAP-treated mice, contrary to controls. Muscle immunohistology confirmed the presence, in control mice, of a strong $CD8^+$ T cell infiltrate detected as disseminated brown spots throughout the muscle, while very few or no spots could be seen in MnTBAP-treated and naive mice (PBS/PBS), respectively (Figure 4B, right panels). Concomitantly, spleens of mice were harvested to measure transgene-specific $CD4^+$ and $CD8^+$ T cell responses by the frequency of Dby-or Uty-activated IFN-γ-producing cells, respectively. Preservation of muscle structure along with long-term maintenance muscle transduction in MnTBAP-treated mice correlated with the absence of transgene-specific $CD4^+$ cell response detected at day 8 post-vector injection and the persistence of very low transgene-specific $CD4^+$ and $CD8^+$ T cell immune responses at day 15, compared to control mice (Figures 4F and 4G). Hence, MnTBAP treatment appears to

and CD8 (G) cell populations in the spleen. C57BL/6 mice received i.p. multi-injections with MnTBAP or with an equivalent volume of PBS (day 0 to day 4). At days 4, 8, and 16, spleens were harvested and analyzed for cell-surface CD3, CD4, and CD8 expression by flow cytometry. Geometric means of fluorescence for each receptor are expressed relative to the cells from the control PBS-treated mice (PBS, arbitrarily set at 100%). Results are from 2 independent experiments. All statistical analyses were performed using the Mann-Whitney test. $^{**}p < 0.005$.

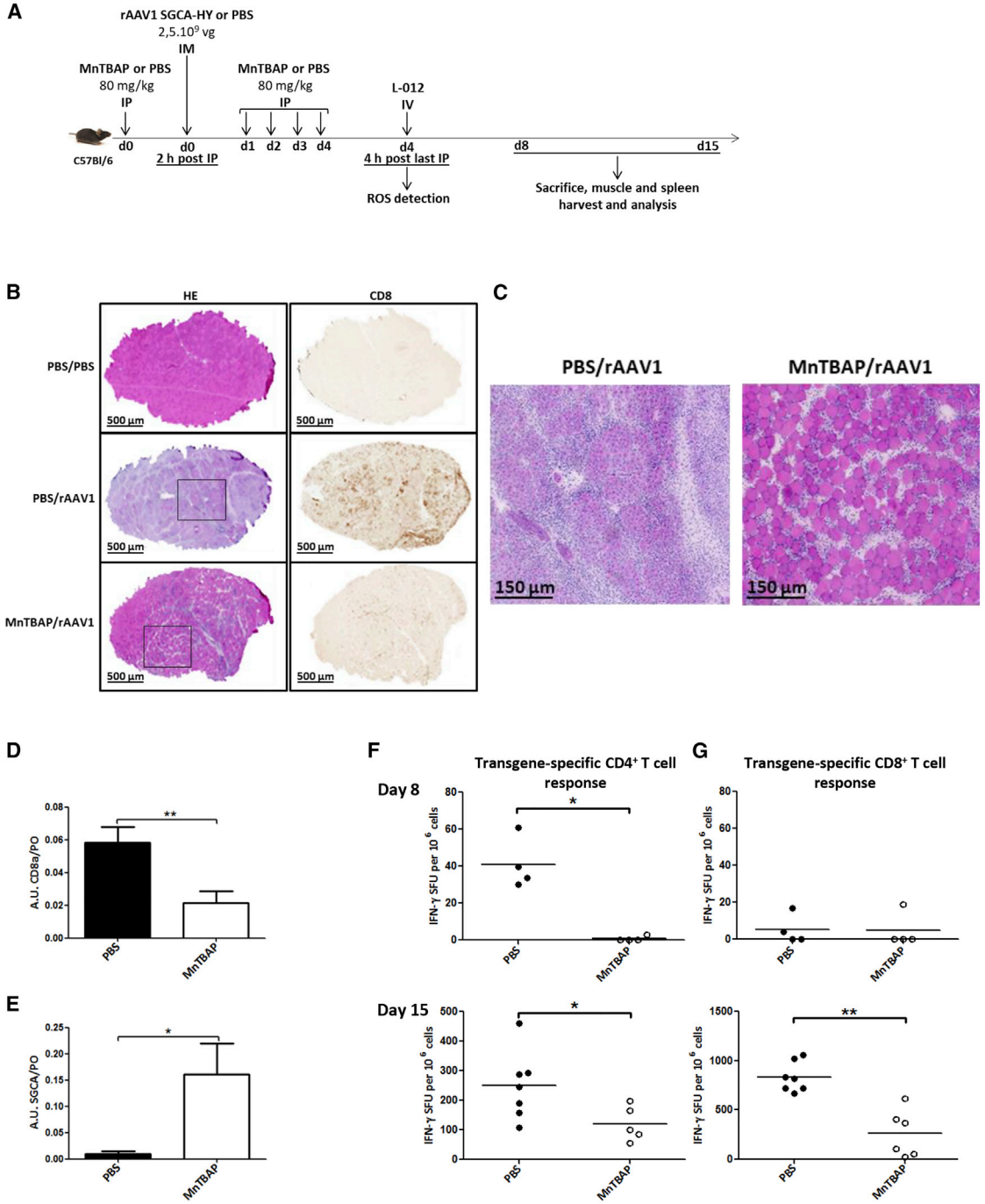

Figure 4. MnTBAP Counteracts the Adverse Effects of rAAV-Mediated i.m. Gene Delivery

(A) Protocol outline. C57BL/6 mice received i.p. multi-injections of MnTBAP or an equivalent volume of PBS (80 mg/kg daily during 5 days). Two hours after the first injection of MnTBAP, mice were administered PBS or rAAV1_CMV_SGCA_HY vector (2.5×10^9 vg per mouse) in the left TA. Four days post-vector injection, mice were intravenously injected with 1.5 mg L-012, a chemical agent that reacts with ROS to produce light. Fifteen days post-rAAV-vector injection, muscle integrity, transgene and CD8a mRNA expression, and transgene-specific T cell responses were analyzed. (B) Histological analysis of injected TA muscle from PBS- or MnTBAP-treated mice, 15 days following injection of rAAV vector or control PBS. Microscopy analysis of cryosections of rAAV-injected muscles after H&E staining (left panel) or anti-CD8 staining followed by enzymatic detection (right panel) was performed. Images are representative of one experiment out of 2, with 3–4 mice per group. Scale bars, 500 µm. (C) High magnifications of selected areas shown in (D). Scale bars, 150 µm. (D and E) Analysis of CD8a and SGCA transgene expression by RT-PCR in injected TA muscle 15 days following injection

(legend continued on next page)

be effective not only at preventing inflammation due to its intrinsic antioxidant property but also at impairing $CD4^+$ T cell responses and decreasing $CD8^+$ T cell infiltrate and cytotoxicity against transgene. In this manner, MnTBAP allowed muscle structure preservation and sustained transgene expression in skeletal muscle.

MnTBAP Attenuates Humoral Response against Capsid Allowing Effective Transduction upon Readministration of Vectors of the Same Serotype

A notable obstacle for gene therapy using rAAV vectors is the induction *in vivo* of capsid-specific $CD4^+$ and $CD8^+$ T cell responses and anti-AAV neutralizing antibodies (NAbs), which not only may limit the duration of transgene expression following AAV gene transfer but also can completely prevent transduction of a target tissue when administering the same serotype.[23] The induction of antibodies to the AAV caspid is dependent upon innate immune activation and involves TLR9-mediated $CD4^+$ T cell activation into TH1 effector cells.[24,25] To assess the effects of MnTBAP on the induction of anti-capsid antibodies following rAAV gene transfer, we designed a protocol in which the rAAV vector was this time intravenously (i.v.) injected to favor a higher exposure to the vector material of lymphoid tissues, which are critically involved in antigen presentation and in the initiation of the immune response to capsids, and rechallenged the mice with local i.m. injections of an rAAV bearing the same capsid serotype but a different transgene (Figure 5A). MnTBAP treatment for 5 consecutive days (days 0 to 4) at the same time as vector administration (day 0) successfully attenuated humoral immunity to viral capsid, since MnTBAP-treated mice produced no or significantly less specific anti-rAAV immunoglobulin G (IgG) compared to the control group, respectively, at day 21 and day 28 post-vector injections (Figures 5B and 5C). A second rAAV was injected 28 days after primary vector exposure (Figure 5A). The second vector bears the same serotype but encodes a secreted form of murine alkaline phosphatase (mSEAP) that can be quantified in blood samples as well as on tissue sections. The level of secondary-type anti-rAAV1 antibody titers, measured 10 days following vector reexposure (day 38), in the MnTBAP cohort was significantly lower compared to that in the control PBS group (Figure 5D). In addition, a higher transduction efficiency of injected muscle was observed, since a significant amount of mSEAP-positive fibers was detected, around 3 months after vector reexposure in the injected-TA muscle sections of MnTBAP-treated primed mice (TA MnTBAP/rAAV1) (Figure 5E). The amount of mSEAP-positive fibers observed was comparable to that in the positive control group of PBS-treated mice that had not been exposed to rAAV1 vector before mSEAP vector administration (TA PBS/PBS) (Figure 5E). In contrast, similarly to contralateral non-injected muscles that did not stain at all (contralateral TA), only very few mSEAP-positive fibers could be seen in muscle sections of PBS-treated mice that had been primed with rAAV1 vector (TA PBS/rAAV1) and reinjected with mSEAP vector (Figure 5E). As expected, the levels of circulating mSEAP correlated with the number of muscle fibers positive for mSEAP (Figure 5F). Likewise, a significantly higher copy number of the readministrated vg was detected, 3 months after vector reexposure, in the injected-TA muscles of MnTBAP-treated mice compared to those of control mice (Figure 5G). Altogether, these results indicate that one short period of treatment with MnTBAP at the time of primary vector exposure appears to be effective at attenuating memory humoral immunity to rAA1 capsid proteins to levels that allow efficient preservation of a second vector of the same serotype from neutralization upon reexposure. That was not the case for PBS-treated primed mice, in which, upon secondary response to the same antigen, memory cells might have been rapidly activated[26] to produce NAbs to bind to the AAV capsid, resulting in the reduction of transduced target cells (Figures 5E and 5F).

DISCUSSION

Our data show for the first time that the synthetic anti-oxidant MnTBAP effectively, rapidly, and reversibly deprives T cells of extracellular membrane CD4 and, to a lesser extent, of CD8 and that this has functional antiviral or immunomodulatory impacts. Indeed, MnTBAP treatment of T cells prevents CD4-dependent gp120-mediated lentiviral transduction. *In vivo*, repeated administration of MnTBAP in mice prevents the induction of antigen-specific TH1 T cell responses and the production of neutralizing antibodies to rAAV.

The effects of MnTBAP on the downregulation of CD4 and CD8 are novel, since MnTBAP is otherwise known as a superoxide dismutase mimetic that prevents the induction of ROS. The mechanism involved here is rapid (maximum, 2 min) and leads to the internalization of cell-surface CD4 into clathrin-coated pits with possible re-expression at the membrane within hours up to a full recovery in less than a day. The mechanism concerns CD4 and CD8, but membrane levels of CD3 were unchanged. Upon antigenic recognition, TCR signaling is initiated by the phosphorylation of TCR tyrosine residues by a pool of pre-activated $p56^{Lck}$ present in the cells,[27] and subsequent protein-protein interactions between $p56^{Lck}$ and CD4 promote the distribution of $p56^{Lck}$ to the TCR-peptide-MHC complex in the immunological synapse.[28] $p56^{Lck}$ and its localization to the plasma membrane of T cells were not altered by MnTBAP treatment. However, the CD4/$p56^{Lck}$ complex was disrupted. It is known that naive peripheral T cells from $Lck^{-/-}$ mice exhibit a normal phenotype, with the exception of reduced levels of CD4 on the cell surface,[29] and that myeloid cells lacking $p56^{Lck}$ expression exhibit significant constitutive CD4 endocytosis.[30] Therefore, it is not clear at this point whether MnTBAP disrupts the CD4/$p56^{Lck}$, which causes internalization of CD4, or whether MnTBAP causes CD4 internalization, which dissociates the complex. MnTBAP was effective not only on murine cells but also on human cells in drastically reducing

of rAAV vector or control PBS. Levels of CD8a (D) and SGCA (E) mRNA are expressed in arbitrary units (AU) relative to the endogenous murine acidic ribosomal phosphoprotein (PO) mRNA (n = 2; 3–4 mice per group). (F and G) Analysis of transgene-specific T cell responses: 8 days (upper panels) and 15 days (lower panels) post-injection of vector, splenic cells were harvested to measure the frequency of transgene specific $CD4^+$ (F) and $CD8^+$ (G) T cells by IFN-γ ELISPOT. Dots represent individual mice. Horizontal bars indicate the average values. All statistical analyses were performed using the Mann-Whitney test. $^*p < 0.05$; $^{**}p < 0.005$.

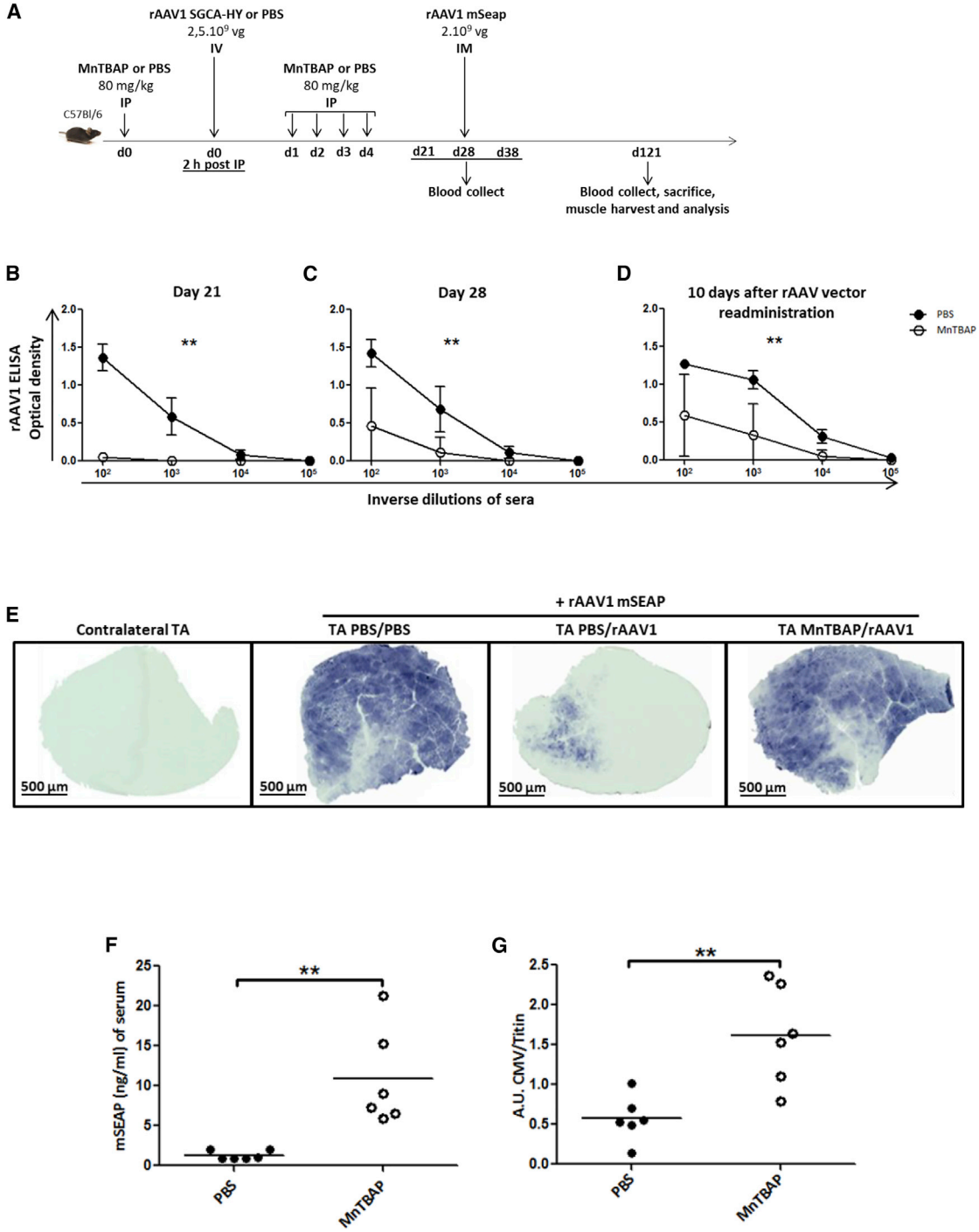

Figure 5. MnTBAP Inhibits Primary and Memory Humoral Response against Capsid Allowing Efficient Readministration of rAAV Vector in Muscle

(A) Protocol outline. C57BL/6 mice received i.p. multi-injections of MnTBAP (80 mg/kg daily during 5 days) or an equivalent volume of PBS. Two hours after the first injection of MnTBAP, mice were administered i.v. injections with PBS or rAAV1_CMV_SGCA_HY vector (2.5×10^9 vg per mouse). Each mouse was subjected to a second injection of rAAV serotype 1 encoding the mSEAP reporter gene (2×10^9 vg of rAAV1_CMV_mSEAP vector per mouse) into the left TA, 28 days after the first injection of vector. (B and C) Analysis of capsid-specific primary humoral response: anti- rAAV1 IgG titers were measured by ELISA in serum samples harvested at day 21 (B) and day 28 (C) post-vector injection. Curves represent the mean ± SD of optical density (OD) obtained at the indicated dilutions of sera from 6 mice per group and compare anti-rAAV IgG response in MnTBAP-treated mice (open circles) with that in PBS-treated mice (closed circles). (D) Analysis of capsid-specific memory humoral response after rAAV1 readministration

(legend continued on next page)

cell-surface CD4 and, to a much lesser degree, cell-surface CD8. The differential effects of MnTBAP on CD4 and CD8 might be explained by a less extensive association of CD8 coreceptor to $p56^{Lck}$ compared to CD4.[31] In mice treated with MnTBAP, the disappearance of CD4 and CD8 was observed at early time points (day 4 but not day 8 or later). Presumably, the reduced CD4 and CD8 levels in T cells were also associated with disrupted interactions between CD4 or CD8 and $p56^{Lck}$, which could have perturbed antigen-induced TCR-mediated signaling and immunological synpase formation. Furthermore, the loss of CD4 localization to microvilli may disturb the initial phase of T cell activation ensured by CD4 as a scanning machinery to select for cells that have MHCII on their surface.[9] Therefore, MnTBAP is expected to inhibit the priming of T cells and the development of B cell responses with reduced effector T cells and antibody-secreting cells. The effects of MnTBAP on CD4 or CD8 downregulation have not yet been described elsewhere to our knowledge. However, MnTBAP is known to reduce acute viral infection when administered daily at a low dose of 5 mg/kg in a murine model of lymphocytic choriomeningitis virus (LCMV) infection.[6] These effects were ascribed to $CD4^+$ T cell death mediated by an altered redox regulation of mitogen-activated protein (MAP) kinases. Our results suggest that LCMV priming defects could also have been induced by MnTBAP in this model.

The induction of immune tolerance is a daunting challenge in many conditions, including solid organ and hematopoietic stem cell transplantation,[32] as well as in gene therapy.[33] Our results provide a novel target for immunomodulatory strategies in gene therapy. In view of the crucial role of the CD4 co- receptor as a target for the onset and the maintenance (memory formation signal) of immune responses,[34,35] the possibility to render this target surface molecule inaccessible during the priming of immune responses, as was shown here with MnTBAP, could be useful. As shown with OVA immunization, the MnTBAP treatment can effectively prevent T cell-mediated immunity but is transient and functionally reversible. Therefore, selective and not generalized immunosuppressive treatment could be devised, which is useful for gene therapy applications. MnTBAP could, thus, still allow the body to react to opportunistic infections contrary to common immunosuppressive drugs,[36] which penalize the entire immune system for unwanted activity of just a small fraction of its lymphocytes. Transient CD4 co-receptor modulation by MnTBAP was evaluated in the context of AAV-mediated gene transfer. Recent studies documented rAAVs as a tool of choice for gene therapy to treat genetic disorders because of their efficiency *in vivo*, leading to the market approval in Europe and the United States of several gene therapy drugs, including a rAAV1-based gene delivery in muscle.[37] rAAVs are non-inflammatory vectors but trigger immune responses to the AAV capsid and/or transgene capable of compromising long-term therapeutic efficacy. Novel strategies are, therefore, needed to be able to readminister the vector after a period of time to maintain therapeutic levels of transgene product in patients.[38] However, the neutralizing anti-capsid antibodies generated by the first rAAV vector administration limit vector redosing.[38] Immunomodulatory or immunosuppressive treatments that enable rAAV redosing present a great interest for gene therapy. Novel immunosuppressive agents such as nanoparticles loaded with rapamycin have been successfully used with rAAV gene delivery preclinical models to reduce rAAV capsid immunogenicity and to enable effective vector readministration.[36] Our study provides another alternative to reduce immune responses induced by rAAV gene transfer using a non-toxic, non-immunosuppressive agent at the time of vector delivery. MnTBAP not only reduced anti-transgene CD4 and CD8 T cell responses preventing muscle fiber destruction but also prevented the establishment of T cell and B cell immune responses against the rAAV1 capsid, enabling redosing with the same serotype. The control of anti-SGCA-HY immune responses obtained with MnTBAP was as efficient as previously obtained in this model by regulating direct antigenic presentation of the transgene using a microRNA 142.3p-regulated cassette.[22] This further argues that MnTBAP acts by blocking the priming of T cell responses against the AAV1 capsid and against the SGCA-HY transgene peptides. Advantageously, a brief period of MnTBAP treatment was sufficient to prevent the establishment of T cell immune memory, allowing for antigen reexposure. MnTBAP is not an approved drug for human use. Thus, further work is warranted to explore the pharmacological and therapeutic properties of MnTBAP or similar compounds, as well as other strategies leading to temporary CD4 downregulation. In addition, not only are the appealing properties of MnTBAP potentially useful for gene therapy, but it may also be exploited for autoimmunity or in any form of active immunopathology associated with excessive or undesirable immune responses.[26]

MATERIALS AND METHODS

Animals

Six- to 8-week-old female C57BL/6 mice were purchased from Charles River Laboratories (L'Arbresle, France). Mice were housed

(rAAV1_CMV_mSEAP vector) in TA. Measurement of anti- rAAV1 IgG titers by ELISA was performed in serum samples from 6 mice per group, harvested 10 days after rAAV vector readministration. For (B)–(D), statistical analyses with the Mann-Whitney test were performed on AUC values, obtained from ODs at four dilution points for each mouse serum. (E) Histochemical detection of mSEAP in injected TA harvested 93 days after vector readministration (day 121). In the first panel, non-injected right contralateral TA is represented as negative control. The second panel shows injected left TA with the rAAV1_CMV_mSEAP vector alone as positive control of mSEAP expression in muscle. The third and fourth panels show administered left TA with the rAAV1_CMV_mSEAP vector in PBS- or MnTBAP-treated mice, respectively, and who received an initial systemic injection of rAAV1_CMV_SGCA_HY vector. Images are representative of one mouse out of 6 per group. Scale bars, 500 μm. (F) Serum level of mSEAP measured by a chemiluminescent assay from mice harvested 93 days after vector readministration (day 121). Dots represent individual mice (closed and open circles show PBS- and MnTBAP-treated mice, respectively). Statistical analyses were performed using the Mann-Whitney test. (G) Copy number analysis of readministered rAAV1 in injected TA by quantitative CMV PCR assay with endogeneous titin gene for normalization. Data are expressed in AUs relative to titin DNA. Each symbol represents a mouse (closed and open circles indicate PBS- and MnTBAP-treated mice, respectively). Statistical analyses were performed using the Mann-Whitney test. $^{**}p < 0.005$.

under specific pathogen-free conditions and handled in accordance with French and European directives. Protocols were conducted according to national and international ethical standards and were approved by the local ethics committee (C2EA-51).

In Vitro and *In Vivo* MnTBAP Treatments

MnTBAP (Calbiochem, San Diego, CA, USA; or Enzo Life Sciences, Farmingdale, NY, USA) was dissolved in 75 mM NaOH to constitute a 20-mM stock solution. MnTBAP was dissolved in the complete medium, used for *in vitro* treatment, containing RPMI 1640 supplemented with 10% heat-inactivated fetal calf serum (FCS), 100 U/mL penicillin/streptomycin, 2 mM glutamax, and 50 μM 2-ME. Hypertonic medium, used to block clathrin-dependent endocytosis, is complete medium supplemented with 0.45 M sucrose. For *in vivo* treatment, the stock solution was diluted with PBS and administered at 80 mg/kg i.p. daily during 5 days. Control animals were injected with equivalent volumes of PBS.

Splenic $CD4^+$ T Cell Isolation and Flow Cytometry Analysis

After mechanic disruption of the spleen, erythrocytes were eliminated by hypotonic shock with ammonium chloride potassium (ACK) lysing buffer. When indicated, splenic cell suspensions were directly submitted, without further purification, to staining with antibodies. $CD4^+$ T cells were isolated from splenic cell suspensions by negative selection using a $CD4^+$ T cell isolation kit (Miltenyi Biotec, Paris, France) followed by autoMACS (Miltenyi Biotec) magnetic sorting, according to the manufacturer's instructions. Purity of isolated $CD4^+$ T cells was usually >95%.

For flow cytometry analysis, cell suspensions were first incubated, for murine cells, with anti-FcγRIII/II (Fc Block 2.4G2, BD Biosciences, Le Pont de Claix, France) monoclonal antibodies (mAbs) or, for human cells, with γ-globulins from human blood (Sigma-Aldrich, St-Quentin-Fallavier, France) for 10 min at 4°C and then stained for 30 min at 4°C in PBS, 0.1% BSA with Fc Block or γ-globulins present, using saturating amounts of the following mAbs: rat anti-mouse CD4-Pacific Blue (RM4-5, BD Biosciences), hamster anti-mouse CD3-APC (145-2C11, BD Biosciences), rat anti-mouse CD8-Alexa Fluor 700 (53-6.7, eBioscience, Paris, France), mouse anti-human CD3-FITC (fluorescein isothiocyanate) (HIT3a, BD Biosciences), mouse anti-human CD4-APC (RPA-T4, BD Biosciences), and mouse anti-human CD8-Pacific Blue (RPA-T8, BD Biosciences). Gates for the different cell populations were set according to their corresponding isotype controls. Cell viability was determined by staining with 7-aminoactinomycin D (7-AAD; Sigma-Aldrich) or Fixable Viability Dye eFluor 780 (eBioscience). When indicated, samples were fixed with 1% paraformaldehyde. Samples were acquired on an LSR II flow cytometer (BD Biosciences), and data were analyzed with DIVA software (BD Biosciences).

CD4 Immunoprecipitation

Cells, harvested after a 2-h culture with or without MnTBAP, were resuspended in solubilization buffer containing 1% NP-40 (Sigma-Aldrich), 0.1 M $(NH_4)_2SO_4$, 20 mM Tris (pH 7.5), 10% glycerol, 25 mM NaF (Sigma-Aldrich), 1 mM Na_3VO_4 (Thermo Fisher Scientific, Villebon-sur-Yvette, France), and 1× protease inhibitor mixture (Roche, Basel, Switzerland). After 30 min of incubation under gentle agitation, cell lysates were centrifuged at 14,000 × *g* for 30 min. Lysates were frozen in aliquots at −20°C or used immediately. Immunoprecipitation was performed by incubation overnight of lysates with rat anti-mouse CD4 (clone GK1.5, BioLegend, San Diego, CA, USA) under gentle agitation at 4°C. The antigen-antibody complex was then added to Protein A/G Resin slurry (Pierce, Thermo Fisher Scientific), incubated with gentle mixing for 2 h at room temperature, and finally microcentrifuged for 30 s. The pellet was washed five times with solubilization buffer, and the immunoprecipitated material was eluted by incubating the complex for for 2–5 min at 95°C–100°C in Laemmli sample buffer prepared without 2-ME. The immunoprecipitates and whole-cell lysates ("lysates") were electrophoresed in precast SDS-PAGE (10% polyacrylamide) gels (Bio-Rad Laboratories, Hercules, CA, USA), transferred to polyvinylidene fluoride (PVDF) membrane (Merck, Darmstadt, Germany), and probed with anti-$p56^{Lck}$ rabbit antibody (Santa Cruz Biotechnology, Nanterre, France) followed by IRDye conjugated secondary antibody according to the manufacturer's instructions (LI-COR Biosciences, Lincoln, NE, USA). Blots of whole-cell lysates ("lysates") were stripped and reprobed with anti-CD4 (clone GK1.5, BioLegend) antibody and detected using the enhanced chemiluminescence (ECL) method with secondary antibodies coupled to horseradish peroxidase (Pierce). Chemiluminescent signals were digitally acquired with a Chemidoc Imaging System (Bio-Rad, Marnes-la-Coquette, France). Infrared fluorescence of the secondary antibodies was read on an Odyssey Imaging System, and quantification of bands was performed using the ImageStudio Lite software (LI-COR Biosciences).

Immunofluorescence Microscopy

After culture in complete medium with or without MnTBAP at 400 μM, murine splenic $CD4^+$ T cells were collected and subjected to immunostaining as previously described.[7] Briefly, after adhesion on poly-L-lysine-coated slides (Thermo Fisher Scientific), cells were fixed in 4% paraformaldehyde for 5 min at 4°C and for 10 min at room temperature and were permeabilized with methanol for 6 min at −20°C. Cells were stained overnight with rat anti-mouse CD4-APC (BD Biosciences) or with unlabeled primary rabbit anti-mouse clathrin (Abcam, Paris, France) or $p56^{Lck}$ (Santa Cruz Biotechnology) antibodies. These primary antibodies were then detected by staining with the goat anti-rabbit Alexa Fluor 488 or Alexa Fluor 594 secondary antibodies (Invitrogen, Carlsbad, CA, USA) for 30 min at room temperature. Negative controls were performed with the corresponding isotype controls of primary antibodies used. The slides were mounted with DAPI Fluoromount-G (SouthernBiotech, Montrouge, France). Images were acquired with a Leica TCS SP2 DMRE confocal-scanning microscope (Leica Microsystems, Nanterre, France) equipped with 40× and 63× immersion objectives.

Time-Lapse Microscopy

Murine splenic $CD4^+$ T cells were first stained with CFSE, according to the manufacturer's recommendations (Invitrogen) and then with

rat anti-mouse CD4-APC (RM4-5, BD Biosciences) mAb. After staining, cells were incubated in ibidi's μ-Dish (ibidi, Nanterre, France) in the thermo-regulated chamber of the Zeiss Axiovert 100M confocal microscope. A time-lapse acquisition was performed with a delay of 120 s between frames. Each frame was illuminated using 488-nm and 633-nm lasers, and fluorescence was collected using 505- to 580-nm and 644- to 719-nm filters. The magnification was 40×/1.3 oil, and images were saved as 8 bits. The image stack was splitted using ImageJ, v1.43, and images were analyzed using CellProfiler 2.0.10415. The cell segmentation was performed on the CFSE fluorescence, and the fluorescence of the CD4 staining was analyzed using R software. Intensity was normalized to the maximum fluorescence measured at t0 for each condition.

In Vivo Chemiluminescence Imaging of Localized Inflammation

After mouse isofluorane anesthesia, 100 μL L-012 solution (15 mg/mL) (Wako, Osaka, Japan) was administered i.v. in retro-orbital sinus 4 days after the first MnTBAP injection. At 2 min after L-012 administration, mice were placed in an *in vivo* imaging system (IVIS Lumina, PerkinElmer, Waltham, MA, USA), and chemiluminescence images were acquired for each mouse with a typical exposure time of 5 min. Images were quantified using LivingImage (PerkinElmer, Waltham, MA, USA) software, by drawing a region of interest (ROI) around the left inferior limb of the mouse. Radiance (ph/s/cm^2/sr) was measured for each ROI.

Culture and Transduction of Human Primary Cells

CD3$^+$ T cells, from peripheral blood of healthy individual donors, obtained from the French Blood Establishment (EFS, Evry, France) following institutional agreements, were purified by positive selection via MACS beads using a magnetic cell sorting system (Miltenyi Biotec). CD3$^+$ T cells were activated for 3 days at 37°C, 5% CO_2 in plates coated with anti-CD3 (10 μg/mL) and anti-CD28 (10 μg/mL) antibodies (both from Miltenyi Biotec) and filled with RPMI 1640 medium supplemented with 10% heat-inactivated FCS, 100 U/mL penicillin/streptomycin, 2 mM glutamax, and 100 IU/mL interleukin-2 (IL-2) (Miltenyi Biotec). Cells were then transferred on retronectin (20 μg/cm^2)-coated plates in the absence or presence of 400 μM MnTBAP, at a density of 2.5×10^5 cells per milliliter for transduction during 6 h with 6×10^7 physical particles (pp) per milliliter of $gp120_{HXB2}$-env pseudotyped lentiviral vectors (a generous gift of Dr. D. Fenard) expressing GFP reporter gene under the control of hPGK (human phosphoglycerate kinase 1). After transduction, cells were washed and further incubated for 72 h in fresh culture medium (RPMI 1640 medium supplemented as described earlier). Cells were then harvested for CD4 (mouse anti-human CD4-PE, M-T466, Miltenyi Biotec) and GFP expression analysis by fluorescence-activated cell sorting (FACS). Transduction efficiency is determined as the percentage of viable (7-AAD$^-$) lymphoid cells expressing GFP (7-AAD$^-$GFP$^+$).The data were normalized to be a percentage of the control value (None) from each experiment.

rAAV1 Vector Production

Recombinant non-replicative, adenovirus-free rAAV1_CMV_SGCA_HY and rAAV1_CMV_mSEAP vector preparations were generated by transient transfection of HEK293 cells with three endotoxin-free plasmids (Macherey-Nagel, Hoerdt, France): (1) the plasmid packaging (pLTR CO2) supplying the AAV2 rep and cap genes of AAV1 encoding the serotype 1 capsid; (2) the plasmid helper (pXX6) providing the adenovirus helper functions; and (3) the plasmid encoding the transgene. For the rAAV1_CMV_SGCA_HY vector, a chimeric transgene (pGG1 SGCA HY) was used, consisting of the human SGCA gene fused to sequences encoding T cell epitopes of the murine HY gene (Dby peptide [NAGFNSNRANSSRSS] presented by I-A^b and the Uty peptide [WMHHNMDLI] presented by H2-D^b) and expressed from the CMV promoter.[22] For the rAAV1_CMV_mSEAP vector, the pGG2-CMV-muSeAP plasmid encoding the mSEAP under the control of the CMV-IE promoter was used.[39] rAAV1 vectors were purified by centrifugation over a CsCl gradient and titered in vg by real-time PCR as previously described.[39] Vector final suspension was tested for endotoxin level and found to be <10 EU/mL.

OVA Peptide s.c. Immunization

A mixture of OVA peptides was administrated in a s.c. injection in mice anesthetized by i.p. injection of xylazine (10 mg/kg) and ketamine (100 mg/kg). $OVA_{257–264}$ (SIINFEKL) (InvivoGen, San Diego, CA, USA) is a class I (Kb)-restricted peptide epitope of OVA presented by the class I MHC molecule (CMH) H-2Kb. $OVA_{323–339}$ (ISQAVHAAHAEINEAGR) (AnaSpec, San Jose, CA, USA) is an H-2b-restricted OVA class II epitope. 100 μg of each peptide emulsified with the same volume of IFA (Sigma-Aldrich) was administered. Controls were injected with PBS-IFA complexes. OVA peptides and PBS-IFA complexes were injected 2 h or 21 days post-first i.p. injection of MnTBAP (or PBS). Eight days post-OVA peptide injection, mice were sacrificed, and spleens were harvested to analyze OVA-specific T cell response.

rAAV1 Vector Delivery

i.m. Injection

Two hours after the first i.p. injection of MnTBAP, mice were anesthetized by an i.p. injection of xylazine (10 mg/kg) and ketamine (100 mg/kg), and 25 μL rAAV1_CMV_SGCA_HY viral preparation containing 2.5×10^9 vg was injected in the left TA muscle. Controls were injected with PBS.

Mice were sacrificed 15 days after vector injection, and the injected muscles were harvested to perform histologic analysis. Spleens were harvested to analyze transgene-specific T cell response.

i.v. Injection

Two hours after the first i.p. injection of MnTBAP, mice were anesthetized by an i.p. injection of xylazine (10 mg/kg) and ketamine (100 mg/kg), and 200 μL rAAV1_CMV_SGCA_HY viral preparation containing 2.5×10^9 vg was injected into retro-orbital sinus or into tail vein. Controls were injected with PBS. Serum samples were harvested at day 21 and day 28 post-vector injection to analyze capsid-specific humoral response.

Readministration Protocol

After the initial i.v. injection of rAAV1_CMV_SGCA_HY vector at day 0 (2 h post-first i.p. injection of MnTBAP), the second rAAV1 injection (2×10^9 vg of rAAV1_CMV_mSEAP) was performed 28 days later in the left TA muscle. Mice were followed up to 93 days after readministration to analyze capsid-specific humoral response and to measure circulating mSEAP from serum samples. Mice were killed 93 days after the second injection of vector. Left and right TA muscles were harvested for histological and enzymatic assay.

Histologic Analysis

Mice were killed at indicated time points. Injected muscles were harvested, snap frozen in isopentane previously chilled in liquid nitrogen, and kept at −80°C until processing. Transverse cryosections (8 μm thick) of the muscles were either stained with H&E to evaluate inflammation and muscle integrity or used for colorimetric immunostaining or for mSEAP detection.

For colorimetric immunodetection of CD8a, cryosections were rehydrated with PBS for 5 min and then incubated 20 min with H_2O_2 to inhibit endogenous peroxidases at room temperature (RT). After washing with PBS, sections were blocked with PBS with 10% goat serum for 30 min and then incubated with 1/40 dilution of a rat monoclonal primary antibody directed against CD8a (Thermo Fisher Scientific) for 1–2 h at RT. After washing with PBS, sections were incubated with secondary antibody goat anti-rat conjugated with horseradish peroxidase (HRP) (Invitrogen) diluted 1/600 for 1 h at RT. Sections were washed three times with PBS and then incubated with diluted diaminobenzidine (Dako, Trappes, France) for 2–5 min. Then, sections were successively treated with ethanol (5 min), twice in xylene (5 min), and mounted with Eukkit (Labonord, VWR International, Fontenay-sous-Bois, France). The slides were examined with a Nikon microscope (Champigny sur Marne, France). Digital images were captured using a charge-coupled device (CCD) camera (Sony) and processed using Cartograph 5.5 (Microvision Software; Microvision, Evry, France).

For mSEAP histochemical detection, transverse cryosections of TA muscles were fixed in 0.5% glutaraldehyde and washed twice with PBS. Endogenous alkaline phosphatase was heat inactivated for 30 min at 65°C. Sections were then incubated for 5 h at 37°C in 0.165 mg/mL 5-bromo-4-chloro-3-indolyl phosphate and 0.33 mg/mL of nitroblue tetrazolium in 100 mM Tris-HCl, 100 mM NaCl, and 50 mM $MgCl_2$. Sections were counterstained with Nuclear Fast Red.

Measure of Transgene and CD8 Expression by Real-Time RT-PCR

Total RNA was extracted from muscles using TRIzol (Invitrogen). Residual DNA was removed from the samples using the Free DNA removal kit (Ambion, Courtaboeuf, France). cDNA was synthesized from 1 μg RNA using a mix of random hexamers and anchored oligo(dT) 3:1 according to the protocol for the Thermo Scientific Verso cDNA Synthesis Kit (Thermo Fisher Scientific). Real-time PCR was performed using the ABI PRISM 7900 system (Life Technology, Saint Aubin, France) with 0.2 μM of each primer and 0.1 μM of the probe according to the protocol for the ABsolute qPCR ROX Mix (Thermo Fisher Scientific). The primer pairs and TaqMan probes used for ha-sarcoglycan amplification were as follows: 920hasarco.F: 5′-TGCTGGCCTATGTCATGTGC-3′, 991hasarco.R: 5′ TCTGGATGTCGGAGGTAGCC-3′, and 946hasarco.P: 5′-CGGGAGGGAAGGCTGAAGAGAGACC-3′. The ubiquitous acidic ribosomal phosphoprotein (PO) gene was used to normalize the data across samples. The primer pairs and TaqMan probe used for PO mRNA amplification were as follows: m181PO.F: 5′-CTCCAAGCAGATGCAGCAGA-3′, m267PO.R: 5′-ACCATGATGCgCAAGGCCAT-3′, and m225PO.P: 5′-CCGTGGTGCTGATGGGCAAGAA-3′. The primer pairs and TaqMan probes for the mouse CD8a were Mm01182107_g1 (Thermo Fisher Scientific).

Genomic DNA Extraction and Quantitative Real-Time PCR

Genomic DNA was extracted from frozen muscles using a MagNA Pure 96 Instrument (Roche). Real-time PCR to amplify CMV in relation to the titin gene was performed using the ABI PRISM 7900 system (Life Technology, Saint Aubin, France) with 0.1 μM of each primer and 0.1 mM of the probe according to the protocol for the ABsolute qPCR ROX Mix (Thermo Fisher Scientific, Cambridge, UK). The primer pairs and TaqMan probes used for CMV and titin gene amplification were as follows: mTitin-F: 5′-AAAACGAGCAGTGACGTGAGC-3′, mTitin-R: 5′-TTCAGTCATGCTGCTAGCGC-3′, and mTitin-P: 5′-TGCACGGAAGCGTCTCGTCTCAGTC-3′; mCMV-F: 5′-CATCAATGGGCGTGGATAGC-3′, mCMV-R: 5′-GGAGTTGTTACGACATTTTGGAAA-3′, and mCMV-P: 5′-ATTTCCAAGTCTCCACCC-3′. Results were calculated from a standard curve based on dilutions of 2 plasmids containing either the Titin or CMV sequences. Background levels ranged between 36 and 40 CT values.

IFN-γ ELISPOT

Spleens were harvested to analyze the cellular immune anti-transgene response by T cell cytokine response assay. MultiScreen-HA Assay System 96-well filtration plates (Merck) were coated overnight with 2.5 μg/mL anti-mouse IFN-γ purified mAbs (eBioscience) at 4°C, washed, and then blocked with RPMI 1640 medium (Life Technologies, Saint Aubain, France) supplemented with 10% heat-inactivated FCS (Life Technologies), 100 U/mL penicillin/streptomycin (Thermo Fisher Scientific), and 2 mM GlutaMAX-I (Life Technologies) for 2 h at 37°C. Plates were washed three times with RPMI 1640 medium without FCS. Splenocytes were added in duplicate to the IFN-γ-coated well (1 or 0.5×10^6 cells per well) and cultured in the presence of Dby and Uty peptides (GENEPEP, Montpellier, France) at 2 μM or in the presence of OVA peptides at 10 μg/mL. As a positive control, cells were stimulated with concanavalin A (Sigma-Aldrich) at 1 μg/mL in each test. After 24 h, plates were washed three times with PBS and 0.05% Tween 20 and three times with PBS alone before a 2-h incubation at RT with 1 μg/mL biotinylated anti-mouse IFN-γ mAb in PBS/0.1% BSA. Plates were washed three times with PBS/0.05% Tween 20 and three times with PBS alone before

incubation for 1 h and 30 min with 0.66 U/mL streptavidin-alkaline phosphatase (AP) conjugate (Roche Diagnostics, Mannheim, Germany) at RT. After wash step with PBS/0.05% Tween 20, and with PBS alone, spots were developed using BCIP/NBT-plus (Mabtech, Nacka Strand, Sweden). Spots were counted using an AID reader (Cepheid Benelux, Louven, Belgium). Spot-forming units (SFUs) per million cells for each mouse were calculated as the average value of duplicate measures after subtraction of background values obtained with *in vitro* unstimulated splenocytes.

Measurement of Anti-AAV1 Antibody Titers

rAAV1-specific serum antibody titers were evaluated by ELISA. F96 Nunc Maxisorp Immuno Plates (Thermo Fisher Scientific) were coated overnight at 4°C with 0.2×10^9 vg of AAV1 vector diluted in 0.1 M carbonate coating buffer (pH 9.6). Plates were washed three times and blocked with a solution of 6% milk in PBS for 2 h at RT. Serial dilutions of samples in this blocking buffer (10-fold dilutions starting 10^{-2} to 10^{-5} were tested) were incubated on the plates for 1 h at 37°C. Plates were washed three times, incubated with a horseradish-peroxidase-conjugated goat antibody directed against mouse IgG (Southern Biotech, Birmingham, AL, USA), and revealed by the TMB Substrate Reagent Set (BD Biosciences). Reaction was stopped with an H_2SO_4 solution, and the optical density at 450 nm was determined using a luminometer (Discovery HT-R, BioServ, Thiais, France) with KC4 software. The area under the curve (AUC) values obtained from the optical densities at four dilution points were calculated for statistical analysis using GraphPad Prism software (Logi Labo, Paris, France).

Quantification of Circulating mSEAP

Determination of alkaline phosphatase concentration in immunized mice sera was performed by chemiluminescence analysis.[39] Blood samples were centrifuged for 10 min at 8,000 rpm to collect sera, endogenous alkaline phosphatase was heat inactivated for 5 min at 65°C, and the heat-resistant mSEAP was measured by addition of the reaction buffer and CSPD chemiluminescent substrate, according to the manufacturer's instructions (Tropix, Applied Biosystems, Foster City, CA, USA). Chemiluminescence was quantified using an EnSpire luminometer (PerkinElmer, Waltham, MA, USA). Expression levels are expressed as nanograms of mSEAP per milliliter of serum using a standard curve of purified human placental alkaline phosphatase.

Statistics

Statistical analyses were performed using GraphPad Prism 5 software. For antibody production, differences were analyzed by comparing the average values of the AUC for the titration of each mouse serum. Significant differences were defined with probability values inferior to 0.05 (*$p < 0.05$, **$p < 0.005$, and ***$p < 0.001$).

SUPPLEMENTAL INFORMATION

Supplemental Information can be found online at https://doi.org/10.1016/j.omtm.2019.06.011.

AUTHOR CONTRIBUTIONS

A.G. and T.M.A.N.-N. designed the study. S.D.R., J.B., F.O., J.C., G.C., and J.P. performed experiments. D.F. and B.G. provided experimental materials and expertise. S.D.R. and T.M.A.N.-N. analyzed data. A.G. provided the resources for the study. T.M.A.N.-N. and A.G. wrote the manuscript.

CONFLICTS OF INTEREST

The authors declare no competing interests.

ACKNOWLEDGMENTS

We are grateful to Généthon support groups for help with animal care, animal experiments, histology, and rAAV vector production. We would like to thank Armelle Viornery, Maxime Ferrand, Julie Vendomele, Christophe Georger, and Ababacar Khalil Seye for technical assistance and Andràs Paldi for helpful discussions.

REFERENCES

1. Patel, M., and Day, B.J. (1999). Metalloporphyrin class of therapeutic catalytic antioxidants. Trends Pharmacol. Sci. *20*, 359–364.
2. Amarnath, S., Dong, L., Li, J., Wu, Y., and Chen, W. (2007). Endogenous TGF-beta activation by reactive oxygen species is key to Foxp3 induction in TCR-stimulated and HIV-1-infected human CD4+CD25- T cells. Retrovirology *4*, 57.
3. Liu, D., Shan, Y., Valluru, L., and Bao, F. (2013). Mn (III) tetrakis (4-benzoic acid) porphyrin scavenges reactive species, reduces oxidative stress, and improves functional recovery after experimental spinal cord injury in rats: comparison with methylprednisolone. BMC Neurosci. *14*, 23.
4. Suresh, M.V., Yu, B., Lakshminrusimha, S., Machado-Aranda, D., Talarico, N., Zeng, L., Davidson, B.A., Pennathur, S., and Raghavendran, K. (2013). The protective role of MnTBAP in oxidant-mediated injury and inflammation in a rat model of lung contusion. Surgery *154*, 980–990.
5. Cui, Y.Y., Qian, J.M., Yao, A.H., Ma, Z.Y., Qian, X.F., Zha, X.M., Zhao, Y., Ding, Q., Zhao, J., Wang, S., and Wu, J. (2012). SOD mimetic improves the function, growth, and survival of small-size liver grafts after transplantation in rats. Transplantation *94*, 687–694.
6. Crump, K.E., Langston, P.K., Rajkarnikar, S., and Grayson, J.M. (2013). Antioxidant treatment regulates the humoral immune response during acute viral infection. J. Virol. *87*, 2577–2586.
7. Neildez-Nguyen, T.M.A., Bigot, J., Da Rocha, S., Corre, G., Boisgerault, F., Paldi, A., and Galy, A. (2015). Hypoxic culture conditions enhance the generation of regulatory T cells. Immunology *144*, 431–443.
8. Artyomov, M.N., Lis, M., Devadas, S., Davis, M.M., and Chakraborty, A.K. (2010). CD4 and CD8 binding to MHC molecules primarily acts to enhance Lck delivery. Proc. Natl. Acad. Sci. USA *107*, 16916–16921.
9. Glatzová, D., and Cebecauer, M. (2019). Dual role of CD4 in peripheral T lymphocytes. Front. Immunol. *10*, 618.
10. Blazar, B.R., Murphy, W.J., and Abedi, M. (2012). Advances in graft-versus-host disease biology and therapy. Nat. Rev. Immunol. *12*, 443–458.
11. Islam, S.A., and Luster, A.D. (2012). T cell homing to epithelial barriers in allergic disease. Nat. Med. *18*, 705–715.
12. Palmer, M.T., and Weaver, C.T. (2010). Autoimmunity: increasing suspects in the CD4+ T cell lineup. Nat. Immunol. *11*, 36–40.
13. Wood, K.J., and Goto, R. (2012). Mechanisms of rejection: current perspectives. Transplantation *93*, 1–10.
14. Sant, A.J., and McMichael, A. (2012). Revealing the role of CD4(+) T cells in viral immunity. J. Exp. Med. *209*, 1391–1395.
15. Ferrand, M., Galy, A., and Boisgerault, F. (2014). A dystrophic muscle broadens the contribution and activation of immune cells reacting to rAAV gene transfer. Gene Ther. *21*, 828–839.

16. Mays, L.E., Vandenberghe, L.H., Xiao, R., Bell, P., Nam, H.J., Agbandje-McKenna, M., and Wilson, J.M. (2009). Adeno-associated virus capsid structure drives CD4-dependent CD8+ T cell response to vector encoded proteins. J. Immunol. *182*, 6051–6060.

17. Foti, M., Phelouzat, M.A., Holm, A., Rasmusson, B.J., and Carpentier, J.L. (2002). p56Lck anchors CD4 to distinct microdomains on microvilli. Proc. Natl. Acad. Sci. USA *99*, 2008–2013.

18. Heuser, J.E., and Anderson, R.G. (1989). Hypertonic media inhibit receptor-mediated endocytosis by blocking clathrin-coated pit formation. J. Cell Biol. *108*, 389–400.

19. Maxfield, F.R., and McGraw, T.E. (2004). Endocytic recycling. Nat. Rev. Mol. Cell Biol. *5*, 121–132.

20. Piguet, V., Gu, F., Foti, M., Demaurex, N., Gruenberg, J., Carpentier, J.L., and Trono, D. (1999). Nef-induced CD4 degradation: a diacidic-based motif in Nef functions as a lysosomal targeting signal through the binding of beta-COP in endosomes. Cell *97*, 63–73.

21. Wu, L., Shan, Y., and Liu, D. (2012). Stability, disposition, and penetration of catalytic antioxidants Mn-porphyrin and Mn-salen and of methylprednisolone in spinal cord injury. Cent. Nerv. Syst. Agents Med. Chem. *12*, 122–130.

22. Boisgerault, F., Gross, D.A., Ferrand, M., Poupiot, J., Darocha, S., Richard, I., and Galy, A. (2013). Prolonged gene expression in muscle is achieved without active immune tolerance using microrRNA 142.3p-regulated rAAV gene transfer. Hum. Gene Ther. *24*, 393–405.

23. Ertl, H.C.J., and High, K.A. (2017). Impact of AAV capsid-specific T-cell responses on design and outcome of clinical gene transfer trials with recombinant adeno-associated viral vectors: an evolving controversy. Hum. Gene Ther. *28*, 328–337.

24. Rogers, G.L., Suzuki, M., Zolotukhin, I., Markusic, D.M., Morel, L.M., Lee, B., Ertl, H.C., and Herzog, R.W. (2015). Unique roles of TLR9- and MyD88-dependent and -independent pathways in adaptive immune responses to AAV-mediated gene transfer. J. Innate Immun. *7*, 302–314.

25. Sudres, M., Ciré, S., Vasseur, V., Brault, L., Da Rocha, S., Boisgérault, F., Le Bec, C., Gross, D.A., Blouin, V., Ryffel, B., et al. (2012). MyD88 signaling in B cells regulates the production of Th1-dependent antibodies to AAV. Mol. Ther. *20*, 1571–1581.

26. Devarajan, P., and Chen, Z. (2013). Autoimmune effector memory T cells: the bad and the good. Immunol. Res. *57*, 12–22.

27. Nika, K., Soldani, C., Salek, M., Paster, W., Gray, A., Etzensperger, R., Fugger, L., Polzella, P., Cerundolo, V., Dushek, O., et al. (2010). Constitutively active Lck kinase in T cells drives antigen receptor signal transduction. Immunity *32*, 766–777.

28. Rossy, J., Williamson, D.J., and Gaus, K. (2012). How does the kinase Lck phosphorylate the T cell receptor? Spatial organization as a regulatory mechanism. Front. Immunol. *3*, 167.

29. Lovatt, M., Filby, A., Parravicini, V., Werlen, G., Palmer, E., and Zamoyska, R. (2006). Lck regulates the threshold of activation in primary T cells, while both Lck and Fyn contribute to the magnitude of the extracellular signal-related kinase response. Mol. Cell. Biol. *26*, 8655–8665.

30. Raposo, R.A., Trudgian, D.C., Thomas, B., van Wilgenburg, B., Cowley, S.A., and James, W. (2011). Protein kinase C and NF-κB-dependent CD4 downregulation in macrophages induced by T cell-derived soluble factors: consequences for HIV-1 infection. J. Immunol. *187*, 748–759.

31. Bachmann, M.F., Gallimore, A., Linkert, S., Cerundolo, V., Lanzavecchia, A., Kopf, M., and Viola, A. (1999). Developmental regulation of Lck targeting to the CD8 coreceptor controls signaling in naive and memory T cells. J. Exp. Med. *189*, 1521–1530.

32. McDonald-Hyman, C., Turka, L.A., and Blazar, B.R. (2015). Advances and challenges in immunotherapy for solid organ and hematopoietic stem cell transplantation. Sci. Transl. Med. *7*, 280rv2.

33. Mingozzi, F., and High, K.A. (2017). Overcoming the host immune response to adeno-associated virus gene delivery vectors: the race between clearance, tolerance, neutralization, and escape. Annu. Rev. Virol. *4*, 511–534.

34. Phares, T.W., Stohlman, S.A., Hwang, M., Min, B., Hinton, D.R., and Bergmann, C.C. (2012). CD4 T cells promote CD8 T cell immunity at the priming and effector site during viral encephalitis. J. Virol. *86*, 2416–2427.

35. Zhang, S., Zhang, H., and Zhao, J. (2009). The role of CD4 T cell help for CD8 CTL activation. Biochem. Biophys. Res. Commun. *384*, 405–408.

36. Meliani, A., Boisgerault, F., Hardet, R., Marmier, S., Collaud, F., Ronzitti, G., Leborgne, C., Costa Verdera, H., Simon Sola, M., Charles, S., et al. (2018). Antigen-selective modulation of AAV immunogenicity with tolerogenic rapamycin nanoparticles enables successful vector re-administration. Nat. Commun. *9*, 4098.

37. Colella, P., Ronzitti, G., and Mingozzi, F. (2017). Emerging issues in AAV-mediated *in vivo* gene therapy. Mol. Ther. Methods Clin. Dev. *8*, 87–104.

38. Tse, L.V., Moller-Tank, S., and Asokan, A. (2015). Strategies to circumvent humoral immunity to adeno-associated viral vectors. Expert Opin. Biol. Ther. *15*, 845–855.

39. Rivière, C., Danos, O., and Douar, A.M. (2006). Long-term expression and repeated administration of AAV type 1, 2 and 5 vectors in skeletal muscle of immunocompetent adult mice. Gene Ther. *13*, 1300–1308.